

Article

# Apprehensive Drought Characteristics over Iraq: Results of a Multidecadal Spatiotemporal Assessment

Maysoun Hameed <sup>1,\*</sup>, Ali Ahmadalipour <sup>2</sup> and Hamid Moradkhani <sup>1,2</sup>

<sup>1</sup> Department of Civil and Environmental Engineering, Portland State University, Portland, OR 97201, USA

<sup>2</sup> Department of Civil, Construction and Environmental Engineering, University of Alabama, Tuscaloosa, AL 35487, USA; aahmada@ua.edu (A.A.); hmoradkhani@ua.edu (H.M.)

\* Correspondence: mahameed@pdx.edu

Received: 15 December 2017; Accepted: 2 February 2018; Published: 7 February 2018

**Abstract:** Drought is an extreme climate phenomenon that happens slowly and periodically threatens the environmental and socio-economic sectors. Iraq is one of the countries in the Middle East that has been dealing with serious drought-related issues in the 21st century. Here, we investigate meteorological drought across Iraq from 1948 to 2009 at 0.25° spatial resolution. The Standardized Precipitation Evapotranspiration Index (SPEI) has been utilized as a multi-scalar drought index accounting for the effects of temperature variability on drought. Four of the main characteristics of drought including extent, intensity, frequency and duration are studied and the associated spatiotemporal patterns are investigated for each case. Results revealed a significant drought exacerbation over Iraq during the period of 1998–2009. Two significant drought periods of 1998–1999 and 2007–2008 are identified during which severe to extreme droughts covered about 87% and 82% of Iraq, respectively. Analyzing the trends of drought intensity reveals that the central and southwestern parts of Iraq have experienced aggravated intensifying patterns among other regions. In general, droughts are found to be more frequent but shorter at the western, central and southeastern parts of Iraq.

**Keywords:** drought; SPEI; Middle East; Iraq; GLDAS

## 1. Introduction

Drought is an extreme event that happens periodically mostly because of precipitation deficit. Other climatic variables may also contribute to drought occurrence, e.g., temperature, wind, relative humidity and precipitation timing. Drought is considered to be part of the hydrologic cycle since it has devastating impacts on water components such as water supply, water quality, crop yield, surface and subsurface water availability and management of water resources [1–5]. Moreover, drought has a substantial impact on agricultural and economic sectors [6,7].

Drought is generally categorized to four types including: (1) Meteorological drought which is primarily related to precipitation deficit [8–10]; (2) Agricultural drought which is mainly related to soil moisture shortage [11–15]; (3) Hydrological drought which is associated with surface and subsurface water shortfall [16–22]; (4) Socioeconomic drought which is related to a deficiency in the water resources system as a result of the other drought types [1,23–25]. The aforementioned drought types constitute the same process but under distinct phases as a function of time and location [26]. Since the prolonged meteorological drought is considered as the main factor for the occurrence of other types of drought like the agricultural and socioeconomic droughts [27], monitoring meteorological drought may be a preliminary but useful investigation for understanding drought over a certain region.

Several studies have shown that global warming and climate change will aggravate the consequences of drought [28–30]. Dai [30] argued that the atmospheric demand of moisture has increased with the current warming and it has probably changed the atmospheric circulation patterns,

which contributes to drought. Mishra and Singh [31] stated that the rate of global warming has experienced an increasing trend in the past 25 years resulting in an overall increase of extreme events.

Many meteorological drought indices are available in the literature. For example, the Palmer Drought Severity Index (PDSI) [32], the standardized precipitation index (SPI) [33] and the standardized precipitation-evapotranspiration index (SPEI) [34]. Some of these indices, e.g., SPEI or PDSI, account for water balance by incorporating the precipitation and evapotranspiration anomalies and some others are precipitation-based drought indices, e.g., SPI [9]. The PDSI needs calibration to be used in different regions and it can be calculated at fixed time-scales of 9–12 months [34], whereas the SPEI provides the multi-scalar feature. Cook et al. [29] showed that the SPEI is more sensitive to the potential evapotranspiration (PET) than the PDSI in arid regions, e.g., the Sahara and Middle East. Also, Zhang et al. [21] explained that estimating water demand based on PET over arid and semi-arid regions may be unrealistic. Therefore, estimating water demand and also drought quantification can be enhanced by considering PET, runoff and soil moisture [21,22].

Numerous studies have investigated meteorological drought at global scale as well as national or regional scales. For global scale, Dutra et al. [35] presented a probabilistic meteorological drought monitoring methodology based on The European Centre for Medium-Range Weather Forecasts (ECMWF) probabilistic forecasts estimating the SPI. Mo and Lyon [36] applied the North American Multi-Model Ensemble (NMME) to predict the global meteorological drought using the SPI. In another study, the self-calibrated Palmer drought severity index with the Penman–Monteith potential evapotranspiration (sc\_PDSI\_pm) was examined under a low–moderate emissions scenario to analyze the magnitude and key drivers of global drought changes in the twenty-first century [37]. Stagge and Tallaksen [38] compared the SPEI with the SPI over Europe to address the differences among them and to investigate the sensitivity of the SPEI to different potential evapotranspiration (PET) methods. A study by Hoerling et al. [39] assessed droughts in the Mediterranean region by applying global climate models. They showed that drying conditions widely spread from the Atlantic coast to the Middle East during the period of 1971–2010 compared to 1902–1970. In addition, they found that drought frequency has increased after 1970 along with a change toward drier conditions during the cold-season precipitation in the Mediterranean region for the period of 1902–2010. Gleick [40] showed that since 2008, drought frequency and intensity have changed over the eastern Mediterranean region.

Drought has been a characteristic of the Middle East climate [6]. A study in the Eastern Mediterranean and the Middle East (EMME) by Lelieveld et al. [41] showed that the Middle East region is likely to be highly impacted by climate change resulting in more intense and frequent droughts. Iraq, as one of the Middle East countries, has recently experienced drought [42]. Several researchers have studied drought over Iraq [43–46]. AL-Timimi and AL-Jiboori [46] assessed the spatial and temporal changes in drought over Iraq using the SPI for the period of 1980–2010. They found that drought has deteriorated from normal to extreme levels over Iraq during the period of 2000–2010 and 2008 was the driest year. Another study by Robaa and Al-Barazanji [47] showed that after 1995, the rising trend of the annual mean temperature over Iraq is about 0.5 °C/decade. Eklund and Seaquist [45] investigated agricultural drought using the enhanced vegetation index (EVI) in the Duhok Governorate, Iraqi Kurdistan. Their results indicated about 50% decrease in precipitation over the region leading to a 62% reduced vegetated area in 2008. Al-Faraj and Al-Dabbag [43] investigated the combined effects of basin-wide multi-year drought and upstream human-induced activities on the development of the Diyala river basin shared between Iraq and Iran. Recently, a drought analysis was conducted to inspect the Euphrates-Tigris basin located in Iran, Turkey, Iraq and Syria using the SPI drought index [44]. They found that Syria has faced the most severe and frequent droughts in the past 15 years.

The intention of the present study is to utilize a multi-scalar climatic drought index sensitive to global warming (the standardized precipitation evapotranspiration index; SPEI) to study drought over Iraq while addressing the effects of temperature variability on drought. The potential evapotranspiration is calculated using the Thornthwaite method (temperature-based) [48] as an estimate for the water demand in the region. While other studies focused on some parts of Iraq,

the current study covers the entire Iraq and investigates several main spatiotemporal characteristics of drought for the period of 1948–2009.

## 2. Materials and Methods

### 2.1. Study Area and Data

Iraq is located in the southwestern Asia and covers about 435,000 km<sup>2</sup>. A large area of the country is arid and semi-arid regions. Most of the topography is broad plains and the mountains spread in the north and northeastern regions (along the border with Turkey and Iran) (Figure 1). The climate of Iraq varies to be continental and subtropical. Winters tends to be cold (below freezing) with relatively low and uneven precipitation. Precipitation occurs between October and May with higher precipitation amounts falling between December and February. The mean annual precipitation over Iraq is about 154 mm [49]. However, 60% of the country receives less than 100 mm/year (southern parts of Iraq) whereas the mountains regions (north-eastern parts of Iraq) receive the highest amount of precipitation up to 1200 mm/year [49]. Summers are dry, hot in the northern parts and extremely hot (higher than 48 °C) across the rest of Iraq. Spring and fall are very short in Iraq.

Most of the agriculture in Iraq depends on irrigation because of the dry climate, except for the northeastern parts (mountains region) where the rain-fed agriculture is practiced. The Tigris and Euphrates rivers are the main sources of water in Iraq. The two rivers originate from Turkey and enter Iraq from the north and west borders with Turkey and Syria (Figure 1). The Tigris watershed area is about 371,562 km<sup>2</sup> that surrounds about 38% of Iraq. The Euphrates watershed is about 579,314 km<sup>2</sup> and covers about 49% of Iraq [49]. Recently, the amount of water in both rivers has decreased substantially as a result of drought and dam constructions [6].

The Global Land Data Assimilation System Version 2 (GLDAS-2) monthly data with a 0.25° spatial resolution is used in this study [50]. The components of GLDAS-2 are the GLDAS-2.0 that is forced entirely with the Princeton meteorological forcing data and the GLDAS-2.1 that is forced with a combination of model and observation-based forcing datasets. For this study, the monthly precipitation and temperature data were extracted and utilized for 62 years historical period of January 1948 to December 2009.

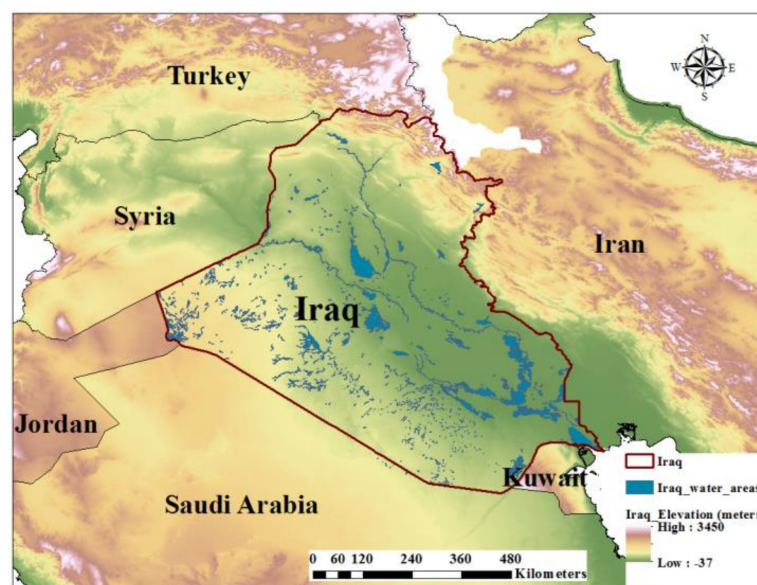


Figure 1. Elevation map of Iraq and neighboring countries (source: <http://www.diva-gis.org>).

## 2.2. Methodology

### 2.2.1. Standardized Precipitation Evapotranspiration Index

The standardized precipitation evapotranspiration index (SPEI) is a multi-scalar drought index which was introduced by Vicente-Serrano et al. [34]. The SPEI is a well-received drought index, which considers two climatic information: precipitation ( $P$ ) and potential evapotranspiration (PET). The SPEI estimates water deficiency ( $D$ ) by considering the difference between the monthly precipitation and potential evapotranspiration ( $P$ -PET). The water deficit ( $D$ ) is the parameter used to explain drought. SPEI is a standardized index that can be calculated at different timescales.

In this study, the accumulation period for SPEI is set to 12 months as an intermediate to long-term analysis. In order to calculate PET, different procedures can be adopted. PET equations can be classified as temperature-based, radiation-based and a combination of both [51]. Four of the most common PET methods are Penman-Monteith (PM) [52], Priestley and Taylor [53], Hargreaves [54] and Thornthwaite [48]. The Penman-Monteith method (PM) is known as a temperature-radiation based method and is considered the standard method for PET estimation by the International Commission on Irrigation and Drainage (ICID), the Food and Agriculture Organization of the United Nations (FAO) and the American Society of Civil Engineers (ASCE). The simple version of (PM) method is the Priestley-Taylor [55]. However, both methods require at least climate data of daily average surface temperature, daily min/max surface temperature and wind speed [51] which are not available with acceptable accuracy for the study region. Nonetheless, Hargreaves and Thornthwaite method are simple methods that are commonly used, as they only require the temperature to calculate PET. Some of the previous studies have indicated that the use of different PET techniques does not show a remarkable effect on drought assessment [56–59]. Mohammed and Scholz [59] mentioned that there are no significant differences of using different PET approaches at low elevations and large time scales of 12 months and above. However, this might not be the case for small periods (e.g., 3, 6 and 9 months) and especially in mountainous regions. Beguería et al. [8] showed that estimating drought indices using different PET methods is still questionable. They also found that using different PET methods to estimate the SPEI series could be significantly larger in semi-arid regions and smaller in humid regions.

Thornthwaite method as described by Vicente-Serrano et al. [34] is applied here for  $0 \leq T \leq 26.5$  °C as shown in Equation (1):

$$PET = 16 \times K \times \left( \frac{10 \times T}{I} \right)^m, \quad (1)$$

where  $T$  is the monthly mean temperature in °C;  $I$  is a heat index, which is calculated from the sum of 12 monthly index values  $i$ , which is derived from the mean monthly temperature;  $K$  is a correction coefficient as a function of the month and latitude; and  $m$  is a coefficient depending on  $I$ . For  $T \geq 26.5$  °C, PET is determined directly from temperature as shown in Equation (2) [60,61]:

$$PET = (-415.85 + 32.24T - 0.43 \times T^2) * K, \quad (2)$$

In other words, the relationship between PET and  $T$  in hot weather is independent of the overall cold or warm conditions of the annual climate [62].

By calculating PET, the water deficit ( $D$ ) is calculated for the month  $i$  using the formula:

$$D_i = P_i - PET_i, \quad (3)$$

To calculate the SPEI-12, a monthly time-series of water deficit ( $D$ ) is accumulated to 12 months (starting from each month of the year) and then fitted to a probability distribution function. Choosing the most proper distribution for the water deficit is not an easy task and there is a discrepancy among the suggested distributions in different studies [34,51]. Several studies have focused on frameworks for

calculating standardized drought indices and the methodology to calculate the indices have advanced over time. For instance, Stagge et al. [63] demonstrated that the optimal distribution for standardization may vary for different regions. Touma et al. [64] carried out analyses on several drought indices and they also reported varied candidate distributions for different locations. In recent years, more attention has been given to the non-parametric approaches (e.g., Huang et al. [65]). The calculated drought index value was subject to the chosen distribution in the conventional distribution fitting approaches and it was unbounded resulting in very high or very low values, which could affect long-term trends. The non-parametric approach relaxes such issues of the conventional methods and removes the subjectivity in the calculations [7]. Therefore, a non-parametric approach is more practical to use and more suitable for this study since the focus is on all drought types and not only the extreme drought [10]. In this study, the empirical Weibull plotting position [66,67] is used as a non-parametric approach as shown in Equation (4):

$$p(x_i) = \frac{i}{n+1}, \quad (4)$$

where  $n$  is the sample size,  $i$  is the rank of data from the smallest and  $p(x_i)$  is the empirical probability. The final step for obtaining the SPEI is to standardize the outcomes of Equation (4) as shown in Equation (5):

$$SI = \phi^{-1}(p), \quad (5)$$

where  $\phi$  is the standard normal distribution function and  $p$  is the empirical probability from Equation (1). The procedure is applied separately for each month for 692 grid cells covering Iraq. SPEI is then classified into seven categories ranging from extreme drought to extreme wet condition as shown in Table 1.

**Table 1.** Categories of dry/wet classes by the SPEI following McKee et al. [33].

Category	SPEI Values
	(min–max)
Extremely dry	Less than $-2$
Severe dry	$-1.99$ to $-1.5$
Moderate dry	$-1.49$ to $-1.0$
Near normal	$-1.0$ to $1.0$
Moderate wet	$1.0$ to $1.49$
Severe wet	$1.50$ to $1.99$
Extremely wet	More than $2$

### 2.2.2. Drought Characteristics

The following drought characteristics are studied in this study:

- Spatial extent of drought
- Trends of drought intensity
- Frequency of drought (number of drought events)
- Duration of drought

Spatial extent of drought is assessed by calculating the ratio of the number of grids experiencing a certain type of drought (e.g., moderate, severe and extreme drought) to the total number of grids across Iraq. The linear trends of drought intensity are detected for each grid according to SPEI during 1948–2009. Number of drought events is investigated over Iraq during 1948–2009. A drought event is defined when the SPEI falls below  $-1$  (moderate drought condition or worse) and stays within dry threshold for more than two months. Similar procedure has been utilized in previous researches to assess drought frequency (e.g., Ahmadalipour et al. [10] and Van Loon, A. F. [68]). Drought duration is defined for each grid as the accumulative period of dry months experiencing each of the three types of

drought (i.e., moderate, severe and extreme). Therefore, drought duration refers to the total duration of dry period. Since the duration of droughts would vary a lot among different locations and drought events, the focus in this study is on the total drought duration. Lastly, the decadal spatiotemporal variations of PET and P are investigated over Iraq to better understand the effects of these two variables on drought.

### 3. Results

#### 3.1. Spatial Extent of Drought

Time series of decadal drought extent over Iraq is calculated for the three types of drought: moderate, severe and extreme and the results are shown in Figure 2. As it can be seen, the decadal patterns vary towards greater drought extent in the late 1990s and the 2000s. Unlikely, the other decades (1950s, 1960s, 1970s and 1980s) show lower drought extent, which is usually moderate drought covering at most 83.5% of area in the late 1950s with no extreme drought. However, severe drought reaches its maximum in the late 1990s with about 87% drought extent recording the worst drought in Iraq by the end of the 20th century. The 2007–2008 period seems to be the worst drought with about 55–82% of Iraq experiencing extreme drought.

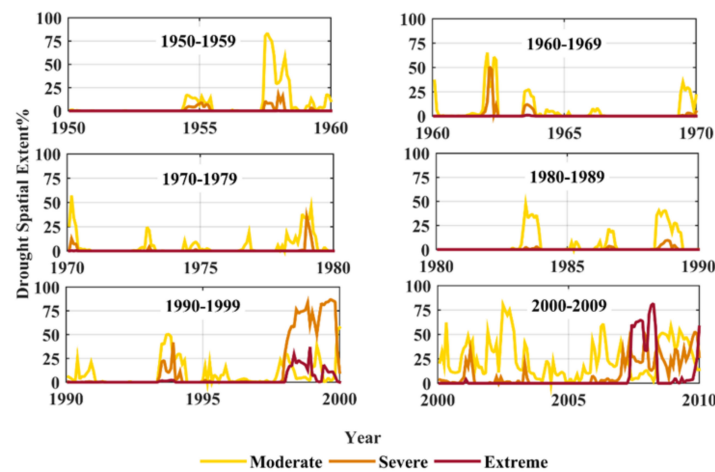


Figure 2. Decadal variations of drought spatial extent over Iraq.

The temporal variations of monthly drought condition ( $SPEI < -1$ ) and wet condition ( $SPEI > 1$ ) are studied by taking the ratio of the number of grids with  $SPEI < -1$  and the grids with  $SPEI > 1$  to the total number of grids in Iraq during the study period of 1948–2009 (Figure 3). From Figure 3, the wet condition governs the period of 1948 to 1997, whereas from 1998 to 2009 dry conditions are being experienced across Iraq.

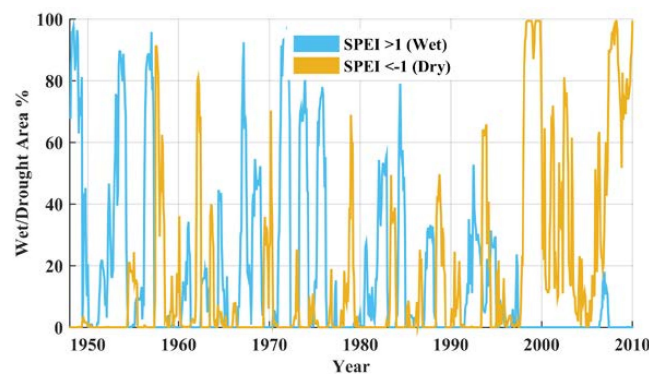
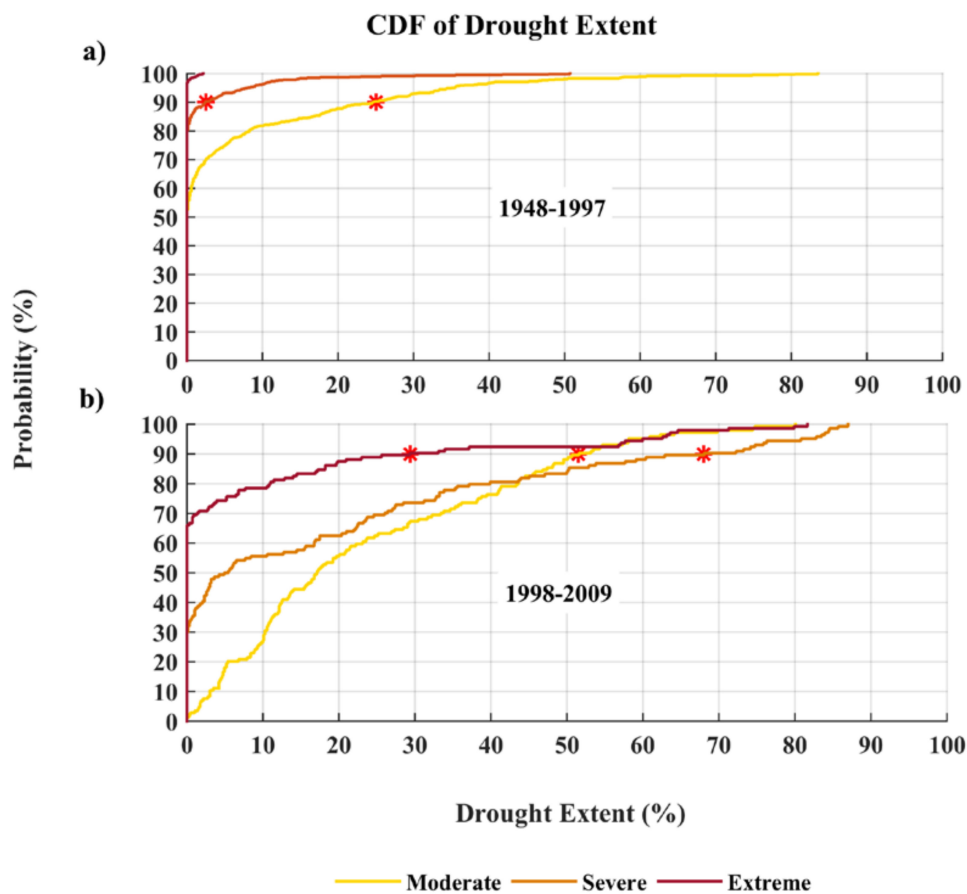


Figure 3. Temporal variations of monthly drought ( $SPEI < -1$ ) and wet ( $SPEI > 1$ ) extent over Iraq.

To better understand the changes in the spatial extent of drought, the probability of SPEI drought extents are plotted for each drought type using the empirical CDF (Figure 4). To generate Figure 4, the time series of drought extent for each drought class is extracted for each period and the cumulative probability distribution (CDF) of drought extent is obtained for each case. The stars refer to the drought extent at the 90th percentile chosen to compare the drought extent of each class between the two periods. In Figure 4, the empirical CDF is presented for two periods of 1948–1997 (wet period) and 1998–2009 (dry period) and the change in the distribution of drought extent is investigated. For the wet period, moderate drought governs about 25% drought extent at the 90th percentile, while severe drought is about 2.5% at the 90th percentile along with no extreme drought. However, the change of probability during the dry period (1998–2009) is more significant and indicates serious drought conditions over the region. Severe drought condition covers an area of about 68% at the 90th percentile. Moderate and extreme droughts show drought extents of about 51.1% and 29.4% at the 90th percentile, respectively.



**Figure 4.** Probability of drought extent based on 12-month SPEI over Iraq for two periods: (a) 1948–1997, (b) 1998–2009.

### 3.2. Trends of Drought Intensity

Understanding the changes in drought intensity is another important step in drought analysis. Therefore, the trends of drought intensity are detected over Iraq according to the SPEI-12. Figure 5 shows the linear trend of SPEI for each grid cell during the study period (1948–2009). A negative trend indicates a decrease in the SPEI and therefore, an aggravation in drought intensity. For example, a trend value of  $-0.01$  indicates that SPEI has decreased about 0.62 during the past 62 years ( $0.01 \times 62 = 0.62$ ) and therefore, drought has intensified. From Figure 5, all the grids across Iraq indicate a slightly negative trend for SPEI (intensification of drought). The most intensified drought trend of  $-0.0026$  is

detected mostly over the mid-west parts of Iraq indicating that SPEI has decreased about 0.16 during the past 62 years. However, the trends are not significant over the other parts of Iraq.

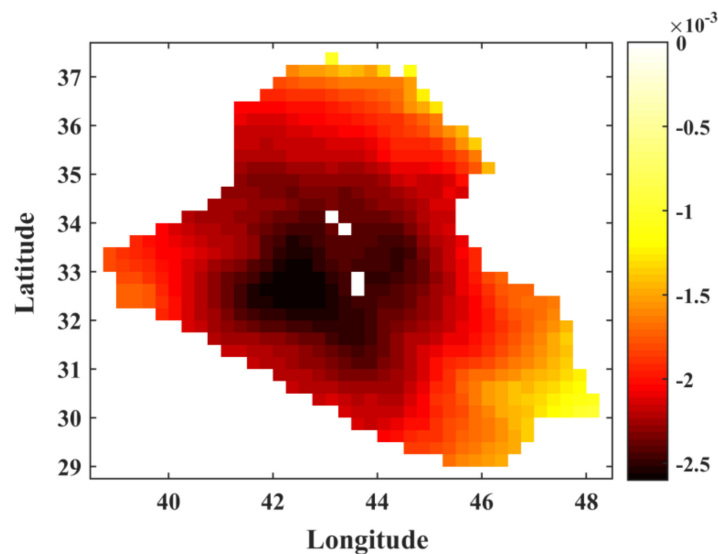


**Figure 5.** Long-term trends of drought intensity for the period of 1948–2009 according to the SPEI-12.

### 3.3. Frequency of Drought

The number of drought events are investigated for each grid for the study period of 1948–2009 and the results are shown in Figure 6. Figure 6 shows the drought occurrence to be more frequent at the western, central and southeastern parts of Iraq. However, the northern and southern parts indicate less frequent drought.

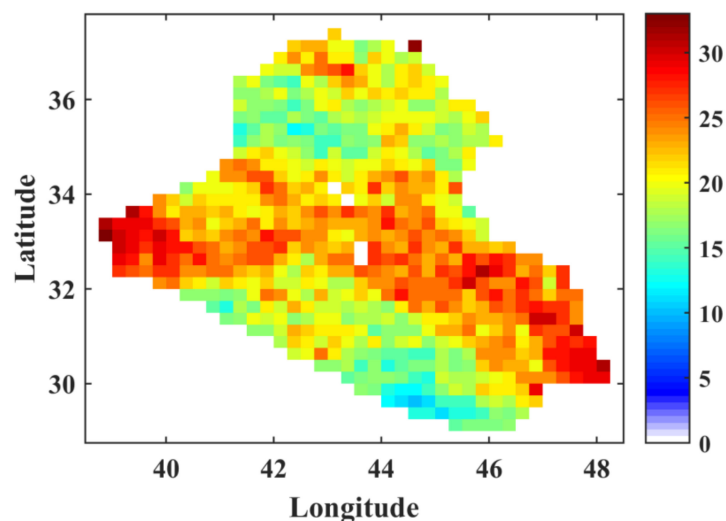


**Figure 6.** Drought frequency across Iraq for the period of 1948–2009 based on SPEI-12.

### 3.4. Duration of Drought

Drought duration is calculated at a monthly timescale for three types of drought, i.e., moderate, severe and extreme, for the period of 1998–2009 and the results are shown in Figure 7. Figure 7 shows that most of the drought that has happened over Iraq during 1998–2009 is moderate drought of up to 56 months at the southwestern parts of Iraq. Severe drought seems to happen similarly across Iraq and most regions have faced about 30 to 36 months of severe drought during 1998–2009. Extreme drought

condition happens rarely, as most of the grids show about 12 months of extreme drought condition in the period of 1998–2009.

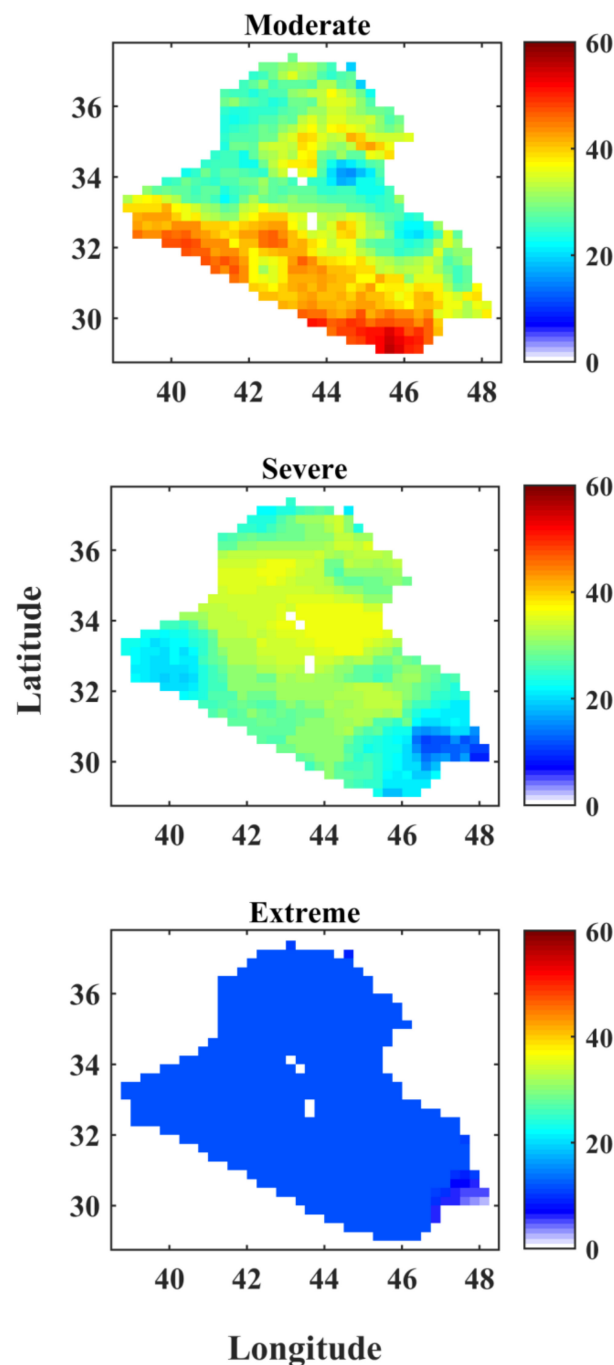


**Figure 7.** Total duration of drought (in months) for the period of 1998–2009 for each drought type: moderate, severe and extreme.

At last, an assessment is carried out by focusing on Iraq as a whole and by generating the time series of the spatially averaged SPEI-12 over Iraq. To do so, the monthly precipitation and temperature data are spatially averaged over Iraq for each month in the study period (1948–2009) and the PET and water deficit ( $D$ ) are calculated for the spatially averaged data to represent the entire Iraq. Then, SPEI-12 is calculated providing a general idea about the fluctuations of dry and wet conditions across Iraq. Figure 8 shows the spatially averaged SPEI results for seven different conditions ranging from

extremely wet (dark-blue color) to extremely dry (red color). The SPEI indicates a substantial decreasing trend (drying pattern) over Iraq. In the late 1950s, severe and moderate drought have occurred with the lowest SPEI values of  $-1.6$  and  $-1.34$ , respectively. Whereas, only moderate droughts have occurred in the 1960s, 1970s and 1980s with the lowest SPEI values of  $-1.45$ ,  $-1.25$  and  $-1.45$ , respectively. The driest periods over Iraq are found to be the late 1990s with the lowest SPEI value of  $-2.4$  (extreme drought) and 2000–2009 with the lowest range of SPEI values of  $-1.96$  to  $-1.74$  for severe drought and a value of  $-2.4$  for extreme drought.

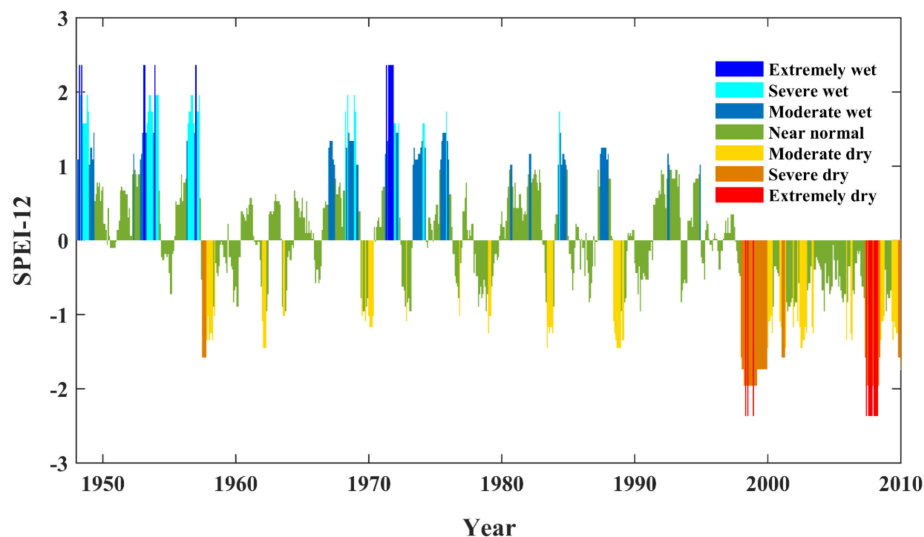


**Figure 8.** Time series of spatially averaged SPEI-12 over Iraq during 1948–2009.

#### 4. Discussion

Many regions in the Middle East have faced serious drought-related challenges in the 21st century, e.g., deficiency of precipitation, lack of irrigation water and diminished water storage [6]. Iraq is one of the Middle East countries that has also been facing serious drought conditions [41]. Therefore, questions may arise about the contribution of the climatic variables in drought occurrence in the region.

In this study, the SPEI was employed to study drought. SPEI accounts for variations in PET and precipitation (P). The literature has proposed the application of PM method for SPEI calculation when data availability is not a limitation, while the Thornthwaite method can be used as an alternative when data is limited [8]. Some studies have discussed that in arid regions, the potential evapotranspiration does not perfectly correlate with the actual evapotranspiration and therefore, the water demand of the SPEI may not accurately capture drought condition [21]. Although it is true for short timescales and flash droughts, researchers have demonstrated that the SPEI correlates with hydrologic drought and streamflow condition at longer timescales [34]. For instance, McEvoy et al. [69] evaluated multiscalar drought indices across Nevada and eastern California and they concluded that SPEI correlates well (correlation coefficient over 0.7) with standardized streamflow at 12 month timescale for most of the studied regions.

In the present study, PET depends on temperature and thus SPEI can be affected indirectly by temperature and directly by PET and P [10]. Therefore, it is of high importance to understand the contribution of these factors on drought. The decadal variations of annual PET and P for the period of 1950–2009 are shown in Figure 9. From Figure 9, PET has increased dramatically in the 1990s and 2000s with the highest PET values of 1349 mm/year and 1374 mm/year, respectively. The increase in PET is found mostly at the central, eastern and southeastern parts of Iraq. These findings are correspondent to drought characteristics results of this study. For instance, drought extent has significantly increased in the late 1990s and most of the 2000s. Furthermore, the spatial pattern of drought frequency (Figure 6)

is reasonably similar to PET. Likewise, PET variation is consistent with drought duration results, especially for moderate and severe drought conditions (Figure 7). From Figure 9, precipitation has decreased noticeably in the northern and northeastern parts of Iraq (the mountains region) and slightly over the rest of Iraq. The lowest amount of precipitation is found during the 1970s and 2000s, i.e., the mean precipitation of 539 mm/year in 1970s and 545 mm/year in 2000s were recorded in northern part of Iraq.

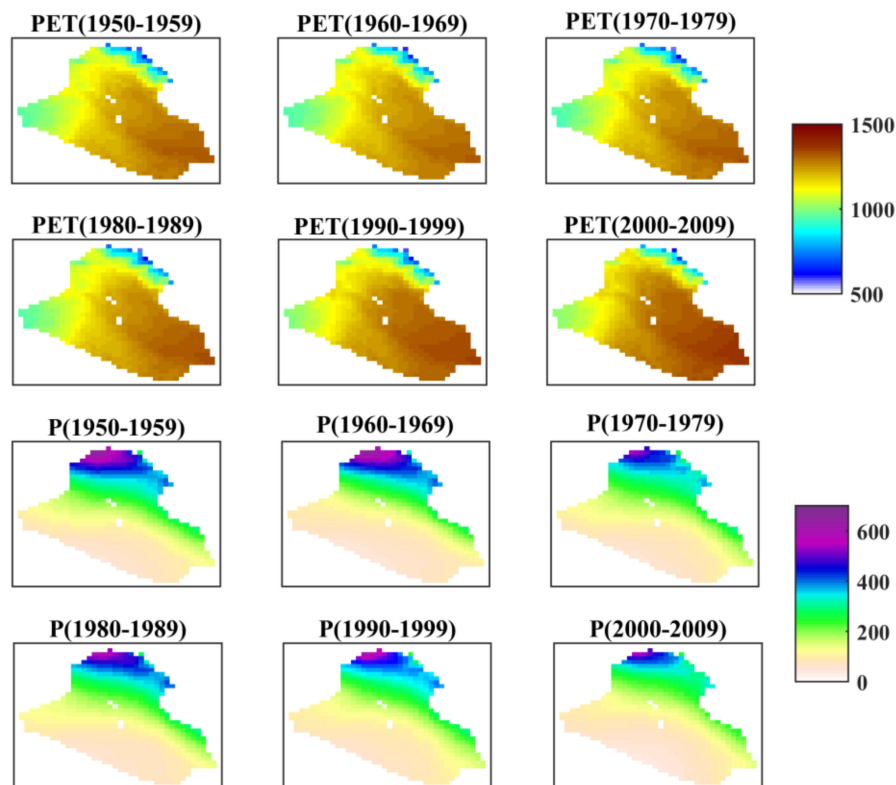


**Figure 9.** Decadal variations of annual potential evapotranspiration (PET) and precipitation (P) over Iraq from 1950 to 2009.

To better understand the impact of each climate variable on drought, the long-term trends of precipitation, temperature and PET are calculated at a monthly timescale and the results are shown in Figure 10. From Figure 10, precipitation has decreased in the northern parts of Iraq. However, temperature has increased over the region mostly on the eastern part of Iraq. Most of Iraq has experienced increasing PET especially in the mid-west parts of Iraq.

Shubbar et al. [70] reported that precipitation has decreased over Iraq and it has been accompanied by very high temperature and dust storms especially in summer when temperature higher than 45 °C has been recorded in Baghdad city (the capital of Iraq) and the southern parts of Iraq. Furthermore, Hoerling et al. [39] showed that the winter precipitation has changed toward drier conditions during the period of 1902–2010 in the Mediterranean region. They explained that after 1970, the drought occurrence has become more frequent over the region. The analysis of precipitation variations of this study (Figure 9) is in accordance with the findings of previous studies, i.e., the decrease in precipitation has occurred in the 1970s over Iraq.

The results of this study revealed a significant drought worsening across Iraq during the period of 1998–2009 versus a mild increase in drought extent for the period of 1948–1997. Gleick [40] reported that the Middle East and North Africa (MENA) region might experience temperature increase and precipitation decrease resulting in worse drought conditions in future.

In this study, two periods of severe drought during 1998–1999 and 2007–2008 were identified over Iraq droughts covered about 87% and 82% of Iraq in those periods respectively. These results are in accordance with the UNESCO report results where the results of SPI-12 showed a significant increase in drought severity during the period of 1999–2011 recording two significant drought years of 1999 and 2008 [42].

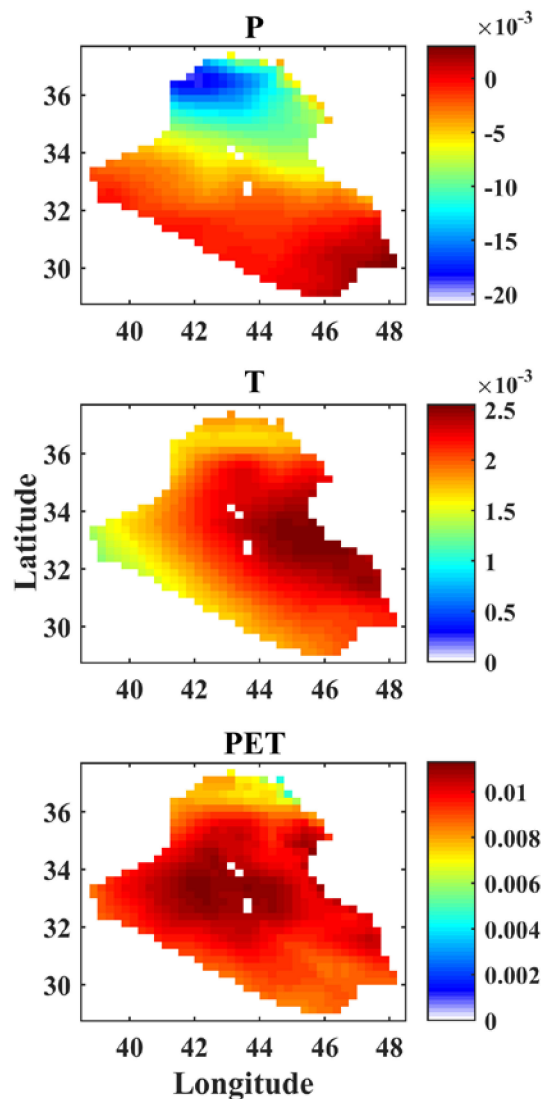


**Figure 10.** Long-term trends of P (mm/month), T ( $^{\circ}$ C/month) and PET (mm/month) for the period of 1948–2009 according to the SPEI-12.

Several other studies over Iraq and the Middle East region have also found similar results. Al-Faraj and Tigkas [71] found that Diyala river basin has suffered from lack of precipitation along with higher temperature and potential evapotranspiration during the multi-year drought periods of 1999–2001 and 2008–2009. A study by AL-Timimi and AL-Jiboori [46] showed that the years 1983, 1990, 1998–2001 and 2007–2009 are the dry years over Iraq and considered years 1999 and 2008 as the driest years according to the SPI drought index. They also mentioned that all drought types occurred increasingly and reached the highest levels during the period of 2000–2010. Moreover, using GRACE it was found by Longuevergne et al. [72] that the Total Water Storage (TWS) in the Tigris-Euphrates basin declined by about  $93 \text{ km}^3$  during the drought period of 2007–2009 in the region. Voss et al. [73] studied the groundwater depletion using GRACE satellite mission in the north-central part of the Middle East.

They also concluded that during the period of 2003–2009, the groundwater usage in Iraq increased due to drought and surface water shortage in the region.

Results of this study showed that drought has become more intense at the central and southwestern parts of Iraq compared to the northern and southeastern parts. Meanwhile, more frequent drought has been experienced at the western, central and southeastern parts of Iraq. In terms of drought duration, moderate drought has been experienced with the longest duration of up to 56 months at the northeastern and southwestern parts of Iraq for the period of 1998–2009. Whereas severe and extreme droughts occurred with the duration of about 30 and 12 months, respectively.

## 5. Conclusions

This study investigated meteorological drought over Iraq during the period of 1948–2009 using a 0.25° reanalysis dataset (GLDAS-2). Four major drought characteristics including drought extent, intensity, frequency and duration were assessed using the SPEI-12 drought index. The main conclusions are summarized as follows:

- A drying trend is detected over Iraq with severe to extreme drought conditions governing the first decade of the 21st century.
- The worst drought condition has occurred during 2007–2008 when severe and extreme drought covered about 25% and 60% of Iraq, respectively.
- The intensity of drought has exacerbated during the past decades, with the most aggravation happening in the central regions of Iraq.
- Droughts are found to be more frequent but shorter at the western, central and southeastern parts of Iraq.

In this study, the historical data were used to investigate various drought characteristics across Iraq. However, climate change is expected to have considerable effects on future drought. Therefore, assessment of future drought conditions using Global Climate Models (GCMs) is of high importance for Iraq, which can be further studied over the region.

**Acknowledgments:** The data used in this study were acquired as part of the mission of NASA's Earth Science Division, archived and distributed by the Goddard Earth Sciences (GES) Data and Information Services Center (DISC).

**Author Contributions:** Maysoun Hameed carried out the analysis and prepared the initial draft of the article. Ali Ahmadalipour contributed in analyzing the data and reviewing the codes and results. Hamid Moradkhani initiated and designed the study and supervised it throughout.

**Conflicts of Interest:** The authors declare no conflict of interest

## References

1. Van Loon, A.F.; Ploum, S.W.; Parajka, J.; Fleig, A.K.; Garnier, E.; Laaha, G.; van Lanen, H.A.J. Hydrological drought typology: Temperature-related drought types and associated societal impacts. *Hydrol. Earth Syst. Sci. Discuss.* **2014**, *11*, 10465–10514. [[CrossRef](#)]
2. Amin, M.T.; Mahmoud, S.H.; Alazba, A.A. Observations, projections and impacts of climate change on water resources in Arabian Peninsula: Current and future scenarios. *Environ. Earth Sci.* **2016**, *75*, 1–17. [[CrossRef](#)]
3. Ahmadalipour, A.; Moradkhani, H.; Yan, H.; Zarekarizi, M. Remote Sensing of Drought: Vegetation, Soil Moisture and Data Assimilation, Remote Sensing of Hydrological Extremes. In *Remote Sensing of Hydrological Extremes*; Springer International Publishing: Basel Switzerland, 2017; pp. 121–149.
4. FAO. *Drought Characteristics and Management in Central Asia and Turkey*; Food and Agriculture Organization of the United Nations: Rome, Italy, 2017.
5. Scanlon, B.R.; Ruddell, B.L.; Reed, P.M.; Hook, R.I.; Zheng, C.; Tidwell, V.C.; Siebert, S. The food-energy-water nexus: Transforming science for society. *Water Resour. Res.* **2017**, *53*, 3550–3556. [[CrossRef](#)]
6. United Nations Development Programme (UNDP). *Impact Assessment, Recovery and Mitigation Framework and Regional Project Design in Kurdistan Region (KR)*; UNDP: Baghdad, Iraq, 2010; p. 78.

7. Ahmadalipour, A.; Moradkhani, H. Analyzing the uncertainty of ensemble-based gridded observations in land surface simulations and drought assessment. *J. Hydrol.* **2017**, *555*, 557–568. [[CrossRef](#)]
8. Beguería, S.; Vicente-Serrano, S.M.; Reig, F.; Latorre, B. Standardized precipitation evapotranspiration index (SPEI) revisited: Parameter fitting, evapotranspiration models, tools, datasets and drought monitoring. *Int. J. Climatol.* **2014**, *34*, 3001–3023. [[CrossRef](#)]
9. Das, P.K.; Dutta, D.; Sharma, J.R.; Dadhwal, V.K. Trends and behaviour of meteorological drought (1901–2008) over Indian region using standardized precipitation-evapotranspiration index. *Int. J. Climatol.* **2015**, *36*, 909–916. [[CrossRef](#)]
10. Ahmadalipour, A.; Moradkhani, H.; Svoboda, M. Centennial drought outlook over the CONUS using NASA-NEX downscaled climate ensemble. *Int. J. Climatol.* **2017**, *37*, 2477–2491. [[CrossRef](#)]
11. Gao, Z.; Xu, N.; Fu, C.; Ning, J. Evaluating Drought Monitoring Methods Using Remote Sensing: A Dynamic Correlation Analysis between Heat Fluxes and Land Cover Patterns. *IEEE J. Sel. Top. Appl. Earth Obs. Remote Sens.* **2015**, *8*, 298–303. [[CrossRef](#)]
12. Mishra, A.K.; Ines, A.V.M.; Das, N.N.; Prakash Khedun, C.; Singh, V.P.; Sivakumar, B.; Hansen, J.W. Anatomy of a local-scale drought: Application of assimilated remote sensing products, crop model, and statistical methods to an agricultural drought study. *J. Hydrol.* **2015**, *526*, 15–29. [[CrossRef](#)]
13. Nichol, J.E.; Abbas, S. Integration of remote sensing datasets for local scale assessment and prediction of drought. *Sci. Total Environ.* **2015**, *505*, 503–507. [[CrossRef](#)] [[PubMed](#)]
14. Vicente-Serrano, S.; Cabello, D.; Tomás-Burguera, M.; Martín-Hernández, N.; Beguería, S.; Azorin-Molina, C.; Kenawy, A. Drought Variability and Land Degradation in Semiarid Regions: Assessment Using Remote Sensing Data and Drought Indices (1982–2011). *Remote Sens.* **2015**, *7*, 4391–4423. [[CrossRef](#)]
15. Yan, H.; Moradkhani, H.; Zarekarizi, M. A probabilistic drought forecasting framework: A combined dynamical and statistical approach. *J. Hydrol.* **2017**, *548*, 291–304. [[CrossRef](#)]
16. Madadgar, S.; Moradkhani, H. A Bayesian Framework for Probabilistic Seasonal Drought Forecasting. *J. Hydrometeorol.* **2013**, *14*, 1685–1705. [[CrossRef](#)]
17. Lorenzo-Lacruz, J.; Vicente-Serrano, S.M.; González-Hidalgo, J.C.; López-Moreno, J.I.; Cortesi, N. Hydrological drought response to meteorological drought in the Iberian Peninsula. *Clim. Res.* **2013**, *58*, 117–131. [[CrossRef](#)]
18. Barker, L.J.; Hannaford, J.; Chiveron, A.; Svensson, C. From meteorological to hydrological drought using standardised indicators. *Hydrol. Earth Syst. Sci.* **2016**, *20*, 2483–2505. [[CrossRef](#)]
19. Van Loon, A.F.; Laaha, G. Hydrological drought severity explained by climate and catchment characteristics. *J. Hydrol.* **2015**, *526*, 3–14. [[CrossRef](#)]
20. Ahmadalipour, A.; Moradkhani, H.; Demirel, M.C. A comparative assessment of projected meteorological and hydrological droughts: Elucidating the role of temperature. *J. Hydrol.* **2017**, *553*, 785–797. [[CrossRef](#)]
21. Zhang, B.; Zhao, X.; Jin, J.; Wu, P. Development and evaluation of a physically based multiscalar drought index: The Standardized Moisture Anomaly Index. *J. Geophys. Res. Atmos.* **2015**, *120*, 11575–11588. [[CrossRef](#)]
22. Mo, K.C.; Lettenmaier, D.P. Objective Drought Classification Using Multiple Land Surface Models. *J. Hydrometeorol.* **2014**, *15*, 990–1010. [[CrossRef](#)]
23. Rajsekhar, D.; Singh, V.P.; Mishra, A.K. Integrated drought causality, hazard, and vulnerability assessment for future socioeconomic scenarios: An information theory perspective. *J. Geophys. Res. Atmos.* **2015**, *120*, 6346–6378. [[CrossRef](#)]
24. Maia, R.; Vivas, E.; Serralheiro, R.; de Carvalho, M. Socioeconomic Evaluation of Drought Effects. Main Principles and Application to Guadiana and Algarve Case Studies. *Water Resour. Manag.* **2015**, *29*, 575–588. [[CrossRef](#)]
25. Huang, S.; Huang, Q.; Leng, G.; Liu, S. A nonparametric multivariate standardized drought index for characterizing socioeconomic drought: A case study in the Heihe River Basin. *J. Hydrol.* **2016**, *542*, 875–883. [[CrossRef](#)]
26. Carrão, H.; Singleton, A.; Naumann, G.; Barbosa, P.; Vogt, J.V. An optimized system for the classification of meteorological drought intensity with applications in drought frequency analysis. *J. Appl. Meteorol. Climatol.* **2014**, *53*, 1943–1960. [[CrossRef](#)]
27. Deo, R.C.; Byun, H.-R.; Adamowski, J.F.; Begum, K. Application of effective drought index for quantification of meteorological drought events: A case study in Australia. *Theor. Appl. Climatol.* **2016**. [[CrossRef](#)]

28. Madadgar, S.; Moradkhani, H. Drought Analysis under Climate Change Using Copula. *J. Hydrol. Eng.* **2013**, *18*, 746–759. [[CrossRef](#)]
29. Cook, B.I.; Smerdon, J.E.; Seager, R.; Coats, S. Global warming and 21st century drying. *Clim. Dyn.* **2014**, *43*, 2607–2627. [[CrossRef](#)]
30. Dai, A. Drought under global warming: A review. *Wiley Interdiscip. Rev. Clim. Chang.* **2011**, *2*, 45–65. [[CrossRef](#)]
31. Mishra, A.K.; Singh, V.P. A review of drought concepts. *J. Hydrol.* **2010**, *391*, 202–216. [[CrossRef](#)]
32. Palmer, W.C. *Meteorological Drought*; US Department of Commerce: Washington, DC, USA, 1965.
33. McKee, T.B.; Doeskin, N.J.; Kleist, J. The relationship of drought frequency and duration to time scales. In Proceedings of the 8th Conference on Applied Climatology, Anaheim, CA, USA, 17–22 January 1993; pp. 179–184.
34. Vicente-Serrano, S.M.; Beguería, S.; López-Moreno, J.I. A Multiscalar Drought Index Sensitive to Global Warming: The Standardized Precipitation Evapotranspiration Index. *J. Clim.* **2010**, *23*, 1696–1718. [[CrossRef](#)]
35. Dutra, E.; Wetterhall, F.; Di Giuseppe, F.; Naumann, G.; Barbosa, P.; Vogt, J.; Pozzi, W.; Pappenberger, F. Global meteorological drought-Part 1: Probabilistic monitoring. *Hydrol. Earth Syst. Sci.* **2014**, *18*, 2657–2667. [[CrossRef](#)]
36. Mo, K.C.; Lyon, B. Global Meteorological Drought Prediction Using the North American Multi-Model Ensemble. *J. Hydrometeorol.* **2015**, *16*, 1409–1424. [[CrossRef](#)]
37. Zhao, T.; Dai, A. The magnitude and causes of global drought changes in the twenty-first century under a low–moderate emissions scenario. *J. Clim.* **2015**, *28*, 4490–4512. [[CrossRef](#)]
38. Stagge, J.; Tallaksen, L. Standardized precipitation–evapotranspiration index (SPEI): Sensitivity to potential evapotranspiration model and parameters. *Int. Assoc. Hydrol. Sci.* **2014**, *10*, 367–373.
39. Hoerling, M.; Eischeid, J.; Perlwitz, J.; Quan, X.; Zhang, T.; Pegion, P. On the increased frequency of mediterranean drought. *J. Clim.* **2012**, *25*, 2146–2161. [[CrossRef](#)]
40. Gleick, P.H. Water, Drought, Climate Change, and Conflict in Syria. *Weather Clim. Soc.* **2014**, *6*, 331–340. [[CrossRef](#)]
41. Lelieveld, J.; Hadjinicolaou, P.; Kostopoulou, E.; Chenoweth, J.; El Maayar, M.; Giannakopoulos, C.; Hannides, C.; Lange, M.A.; Tanarhte, M.; Tyrlis, E.; et al. Climate change and impacts in the Eastern Mediterranean and the Middle East. *Clim. Chang.* **2012**, *114*, 667–687. [[CrossRef](#)] [[PubMed](#)]
42. United Nations Educational, Scientific and Cultural Organization (UNESCO). *Integrated Drought Risk Management—DRM (National Framework for Iraq)*; UNESCO: London, UK, 2014.
43. Al-Faraj, F.A.M.; Al-Dabbagh, B.N.S. Assessment of collective impact of upstream watershed development and basin-wide successive droughts on downstream flow regime: The Lesser Zab transboundary basin. *J. Hydrol.* **2015**, *530*, 419–430. [[CrossRef](#)]
44. Amini, A.; Zareie, S.; Taheri, P.; Bin, K.; Yusof, W.; Raza, M. Drought analysis and water resources management inspection in Euphrates-Tigris basin. In *River Basin Management*; InTech: London, UK, 2016. [[CrossRef](#)]
45. Eklund, L.; Seaquist, J. Meteorological, agricultural and socioeconomic drought in the Duhok Governorate, Iraqi Kurdistan. *Nat. Hazards* **2015**, *76*, 421–441. [[CrossRef](#)]
46. AL-Timimi, Y.K.; AL-Jiboori, M.H. Assessment of spatial and temporal drought in Iraq during the period 1980–2010. *Int. J. Energy Environ.* **2013**, *2*, 653–660.
47. Robaa, S.M.; Al-Barazanji, Z.J. Trends of annual mean surface air temperature over Iraq. *Nat. Sci.* **2013**, *11*, 138–145.
48. Thornthwaite, C.W. An Approach toward a Rational Classification of Climate. *Geogr. Rev.* **1948**, *38*, 55–94. [[CrossRef](#)]
49. The World Bank. *Iraq—Country Water Resource Assistance Strategy: Addressing Major Threats to People’s Livelihoods*; World Bank: Washington, DC, USA, 2006; pp. 1–97.
50. Rodell, M.; Beaudoin, H. GLDAS Noah Land Surface Model L4 Monthly 0.25 × 0.25 Degree V2.0. Available online: [https://disc.sci.gsfc.nasa.gov/datasets/GLDAS\\_NOAH025\\_M\\_V020/summary](https://disc.sci.gsfc.nasa.gov/datasets/GLDAS_NOAH025_M_V020/summary) (accessed on 10 December 2017).
51. Stagge, J.H.; Kohn, I.; Tallaksen, L.M.; Stahl, K. Modeling drought impact occurrence based on meteorological drought indices in Europe. *J. Hydrol.* **2015**, *530*, 37–50. [[CrossRef](#)]

52. Allen, R.G.; Pruitt, W.O.; Wright, J.L.; Howell, T.A.; Ventura, F.; Snyder, R.; Itenfisu, D.; Steduto, P.; Berengena, J.; Yrisarry, J.B.; et al. A recommendation on standardized surface resistance for hourly calculation of reference  $ET_0$  by the FAO56 Penman-Monteith method. *Agric. Water Manag.* **2006**, *81*, 1–22. [[CrossRef](#)]
53. Priestley, C. H.B.; Taylor, R.J. On the Assessment of Surface Heat Flux and Evaporation Using Large-Scale Parameters. *Mon. Weather Rev.* **1972**, *100*, 81–92. [[CrossRef](#)]
54. Hargreaves, G.H.; Samani, Z.A. Reference crop evapotranspiration from temperature. *Appl. Eng. Agric.* **1985**, *1*, 96–99. [[CrossRef](#)]
55. Colaizzi, P.D.; Agam, N.; Tolk, J.A.; Evett, S.R.; Howell, T.A.; Gowda, P.H.; Kustas, W.P.; Anderson, M.C. Two-Source Energy Balance Model to Calculate E, T, and ET: Comparison of Priestley-Taylor and Penman-Monteith Formulations and Two Time Scaling Methods. *Trans. ASABE* **2014**, *57*, 479–498. [[CrossRef](#)]
56. Mavromatis, T. Drought index evaluation for assessing future wheat production in Greece. *Int. J. Climatol.* **2007**, *27*, 911–924. [[CrossRef](#)]
57. Dai, A. Characteristics and trends in various forms of the Palmer Drought Severity Index during 1900–2008. *J. Geophys. Res. Atmos.* **2011**, *116*. [[CrossRef](#)]
58. Vangelis, H.; Tigkas, D.; Tsakiris, G. The effect of PET method on Reconnaissance Drought Index (RDI) calculation. *J. Arid Environ.* **2013**, *88*, 130–140. [[CrossRef](#)]
59. Mohammed, R.; Scholz, M. Impact of Evapotranspiration Formulations at Various Elevations on the Reconnaissance Drought Index. *Water Resour. Manag.* **2017**, *31*, 531–548. [[CrossRef](#)]
60. Willmott, C.J.; Rowe, C.M.; Mintz, Y. Climatology of the terrestrial seasonal water cycle. *J. Climatol.* **1985**, *5*, 589–606. [[CrossRef](#)]
61. Caporusso, N.B.; Rolim, G.D.S. Reference evapotranspiration models using different time scales in the Jaboticabal region of São Paulo, Brazil. *Acta Sci. Agron.* **2015**, *37*, 1–9. [[CrossRef](#)]
62. Hulme, M.; Marsh, R.; Jones, P.D. Global changes in a humidity index between 1931–60 and 1961–90. *Clim. Res.* **1992**, *2*, 1–22. [[CrossRef](#)]
63. Stagge, J.H.; Tallaksen, L.M.; Gudmundsson, L.; Van Loon, A.F.; Stahl, K. Candidate Distributions for Climatological Drought Indices (SPI and SPEI). *Int. J. Climatol.* **2015**, *35*, 4027–4040. [[CrossRef](#)]
64. Touma, D.; Ashfaq, M.; Nayak, M.A.; Kao, S.-C.; Duffenbaugh, N.S. A multi-model and multi-index evaluation of drought characteristics in the 21st century. *J. Hydrol.* **2015**, *526*, 196–207. [[CrossRef](#)]
65. Huang, S.; Huang, Q.; Chang, J.; Zhu, Y.; Leng, G.; Xing, L. Drought structure based on a nonparametric multivariate standardized drought index across the Yellow River basin, China. *J. Hydrol.* **2015**, *530*, 127–136. [[CrossRef](#)]
66. Makkonen, L. Plotting positions in extreme value analysis. *J. Appl. Meteorol. Climatol.* **2006**, *45*, 334–340. [[CrossRef](#)]
67. Weibull, W. A statistical theory of the strength of materials. *R. Swed. Inst. Eng. Res.* **1939**, *151*, 1–45.
68. Van Loon, A.F. Hydrological drought explained. *Wiley Interdiscip. Rev. Water* **2015**, *2*, 359–392. [[CrossRef](#)]
69. McEvoy, D.J.; Huntington, J.L.; Abatzoglou, J.T.; Edwards, L.M. An evaluation of multiscale drought indices in Nevada and Eastern California. *Earth Interact.* **2012**, *16*, 1–18. [[CrossRef](#)]
70. Shubbar, R.M.; Salman, H.H.; Lee, D.I. Characteristics of climate variation indices in Iraq using a statistical factor analysis. *Int. J. Climatol.* **2016**, *37*, 918–927. [[CrossRef](#)]
71. Al-Faraj, F.A.M.; Tigkas, D. Impacts of Multi-year Droughts and Upstream Human-Induced Activities on the Development of a Semi-arid Transboundary Basin. *Water Resour. Manag.* **2016**, *30*, 5131–5143. [[CrossRef](#)]
72. Longuevergne, L.; Wilson, C.R.; Scanlon, B.R.; Crétaux, J.F. GRACE water storage estimates for the middle east and other regions with significant reservoir and lake storage. *Hydrol. Earth Syst. Sci.* **2013**, *17*, 4817–4830. [[CrossRef](#)]
73. Voss, K.A.; Famiglietti, J.S.; Lo, M.; De Linage, C.; Rodell, M.; Swenson, S.C. Groundwater depletion in the Middle East from GRACE with implications for transboundary water management in the Tigris-Euphrates-Western Iran region. *Water Resour. Res.* **2013**, *49*, 904–914. [[CrossRef](#)] [[PubMed](#)]

